JOURNAL OF MATERIALS SCIENCE, 29 (1994) 5673–5679

An anomalous behaviour in the phase stability of the system Fe_2O_3 and NiO

S. RAJENDRAN*, V. SITAKARA RAO
Department of Chemistry, Indian Institute of Technology, Kharagpur 721 302, West Bengal, India

Iron–nickel mixed oxides containing up to 50 mol% of NiO were prepared by firing the corresponding co-precipitated hydrous oxides; characterization was performed by X-ray diffraction, infrared spectroscopy, magnetic susceptibility, electrical conductivity and thermoelectric power measurements. A non-stoichiometric ferrite phase was formed when a sample containing 20 mol% NiO was sintered at 1050 °C. This phase had two- to three-fold higher conductivity than either Fe_2O_3 or the stoichiometric ferrite ($NiFe_2O_4$). The thermoelectric power of this phase indicated a sharp change of charge carriers from n- to p-type near 350 °C. This non-stoichiometric ferrite phase was stable only in a small temperature range and dissociated into α-Fe_2O_3 and stoichiometric ferrite above 1200 °C. Samples containing 5 and 10 mol% NiO also had small fractions of this non-stoichiometric ferrite phase when sintered at 1050 °C.

1. Introduction

Alpha ferric oxide reacts with almost all divalent metal cations and forms the corresponding ferrite spinel ($M^{2+}Fe_2^{3+}O_4$). Relative distributions of these divalent cations in tetrahedral and octahedral lattice sites of the ferrites and the formation of either normal or inverse or mixed ferrites depends upon several factors, such as Madelung energies, ionic radii, the number of d-electrons (in transition metal ions), the covalent nature and site preference energies of the metal cations [1–3]. The chemical nature of these cations, together with the method of preparation and other experimental conditions, also play an important role in determining the temperature at which the stoichiometric ferrite forms and the minimum proportion of divalent cations required to stabilize the ferrite rather than the corresponding solid solution phase [4, 5].

Many investigators have reported [6–9] that in mixed oxide systems containing di- and trivalent metals, excess trivalent metal oxide interacts with the spinel and forms a non-stoichiometric phase at higher sintering temperatures. In MgO–Al_2O_3 system, magnesium aluminate containing up to 82% alumina has been reported [10]. The non-stoichiometric phase has been considered as a solid solution between magnesium aluminate and gamma alumina with cation vacancies as charge compensating defects, i.e. $(MgAl_2O_4)_{1-x}$–$(Al_{8/3}V_{Al,1/3}O_4)_x$ (V_{Al} = aluminium vacancies) [11]. However, the excess alumina separates out during cooling from higher sintering temperatures.

When substituted magnetite is oxidized at low temperature (ca. 350 °C), a superstructure called gamma lacunar (gamma ferric oxide having cation vacancies in the ordered crystallographic lattice sites) has been reported to be formed [7, 12–15]. The stability of the phase is governed by the nature and concentration of the substituents [12, 13] and it undergoes a structural change at higher temperatures. The gamma lacunar phase transforms to alpha ferric oxide if it contains trivalent cations such as Al^{3+} or Cr^{3+} [12, 13]. On the contrary, it dissociates to rhombohedral ferric oxide and ferrite when divalent ions such as Zn^{2+} or Co^{2+} are present in the lattice [16]. No superstructure formation has been reported in the Fe_2O_3–NiO system.

Iron–nickel mixed oxide and nickel ferrite are industrially important and have attracted much attention over the years [1–5, 17–22]. During a course study [17, 23], formation of a non-stoichiometric ferrite phase was observed under a specific set of experimental conditions. The origin and some of the properties of this phase seemed to be different from those generally reported in the literature. Hence, a detailed investigation was undertaken and the observed results are presented here.

2. Experimental procedure

Iron–nickel mixed oxide samples containing up to 50% NiO were prepared by heating the corresponding co-precipitated hydroxides in air in an electric furnace. The hydroxides were prepared from analytical grade nickel nitrate and ferric ammonium sulphate and sodium hydroxide, as reported elsewhere [17, 23].

Hydroxide samples were first heat treated to 550 °C for complete conversion to oxides and then were

* *Present address*: Ceramic Fuel Cells Limited, 710 Blackburn Road, Clayton, Victoria 3168, Australia.

0022–2461

pressed into pellets of 12 mm diameter and 3–8 mm thickness in a hydraulic press at 250–300 MPa. The pellets were then sintered in air in an electric furnace at different temperatures between 1050 and 1300 °C for 4 h. After sintering the specimens were allowed to cool inside the furnace at a controlled heating rate of 500–600 °C. The sintered specimens were ground and powdered samples were investigated.

I.r. spectra of the oxide samples were taken with a grating i.r. spectrophotometer model 577 (Perkin–Elmer) in the range of 4000–200 cm^{-1} using the CsI film technique. The sample to CsI ratio was 1:100–200.

Phase analysis of the specimens was carried out with DRON II (USSR) X-ray diffractometer using filtered iron radiation and a scanning rate of 2° (2 θ) min^{-1}.

Diffraction patterns obtained in a 11.46 cm diameter Debye–Scherrer camera with CrKα radiation were used for the determination of lattice constants. Lattice constants were calculated by the least squares method using a computer program.

Magnetic susceptibility of the specimens was measured with a Gouy balance at room temperature. The field strength was 437.7 A m^{-1}. The Gouy balance was standardized with mercuric cobalt thiocyanate powder. Gram susceptibilities of most of the specimens measured were diluted suitably with alumina for the measurements.

Thermal analyses were carried out using a Derivatograph (Stanton Redcroft) over a temperature range of 20–1400 °C at a heating rate of 20 °C min^{-1}. A 50 mg sample was taken for each run.

3. Results

In this paper FNX indicates an iron–nickel mixed oxide (FN) containing X mol % of NiO. Temperatures, e.g. 550, 750 °C, etc., associated with FNX represent the temperature at which the sample was heat treated or sintered.

The FN20 specimen sintered at 1050 and 1100 °C behaved anomalously compared to other mixed oxides. The anomalous behaviour of this sample is thought to be associated with the formation of a non-stoichiometric ferrite phase. The experimental procedures used to establish this result are set out below.

3.1. I.r. spectral studies

The room temperature i.r. spectra of the specimens (FNX-550 °C) are presented in Fig. 1. Pure ferric oxide (FN0) and FN10 samples show at least five well-defined absorption bands in the oxide region (600–2000 cm^{-1}), which are due to the presence of alpha ferric oxide, the results have been fully explained elsewhere [23]. The spectra of mixed oxide specimens containing > 10 mol % NiO show only two bands. The absorption bands of both FN20 and FN30 are very broad and diffuse and it is very difficult to locate their exact peak positions. The peaks are relatively sharp and well defined for the specimens containing 40 and 50 mol % nickel oxide. In the case of FN50, the

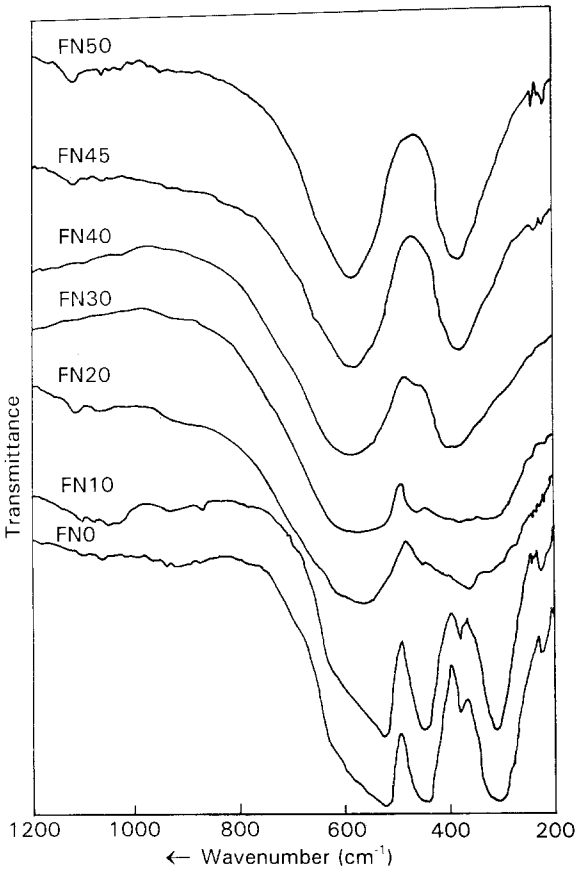

Figure 1 I.r. spectra of iron–nickel mixed oxides containing up to 50 mol % of NiO heated at 550 °C.

bands are centred at 580 and 380 cm^{-1} and they can be attributed to nickel ferrite. The assignment of the observed i.r. frequencies to different modes is quite complex because nickel ferrite is an inverse spinel containing both Ni^{2+} and Fe^{3+} ions in the same octahedral sites. However, it has been reported that the highest frequency bands should be assigned to the higher valent cation [24, 25]. Accordingly, the 580 cm^{-1} band may be assigned to Fe^{3+} –O^{2-} stretching modes of both octahedral and tetrahedral groups since the higher valent Fe^{3+} ions are equally distributed between octahedral and tetrahedral sites. The next lowest frequency band (380 cm^{-1}) can be assigned to the Ni^{2+}–O^{2-} stretching vibration of the octahedral group.

Fig. 2 shows the spectra of FN20 samples either heated to 550–900 °C (curves A–C) for 1 h or sintered at 1050–1300 °C (curves D–F) for 4 h. Curve A has only two absorption peaks which are both very broad and diffuse. Curves B and C show a number of strong absorption peaks at ca. 550, 460, 370 and 330 cm^{-1}, indicating that the 700 and 900 °C calcined specimens contain both alpha ferric oxide and nickel ferrite. The i.r. spectra of specimen sintered at 1200 and 1300 °C (curves E and F) also have many absorption bands in the positions expected for alpha ferric oxide and nickel ferrite, similar to those of the samples heat treated at 700 and 900 °C, revealing that the same two phases are present in these materials.

The FN20-1050 °C spectrum (curve D) has two absorption bands centred at 590 and 400 cm^{-1}. This

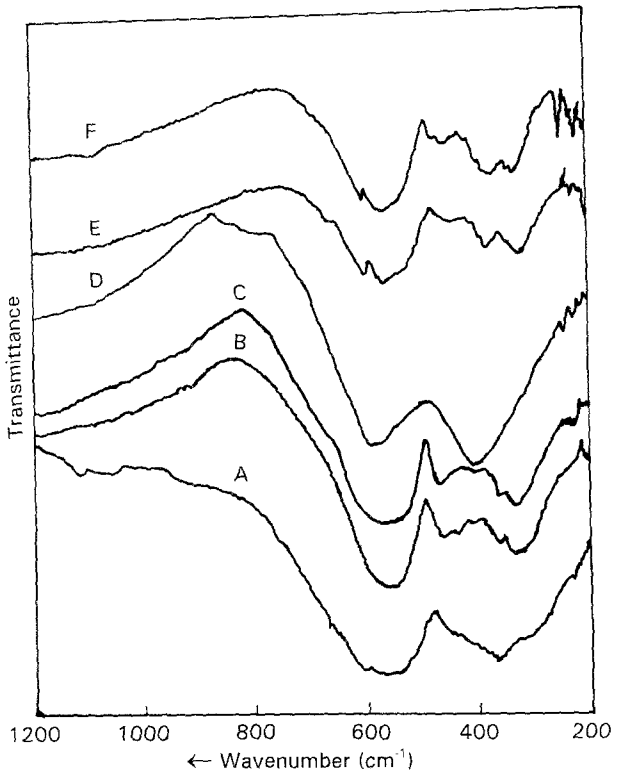

Figure 2 I.r. spectra of FN20 heat treated to different temperatures (°C): (A) 550, (B) 700, (C) 900, (D) 1050 (E) 1200 (F) 1300.

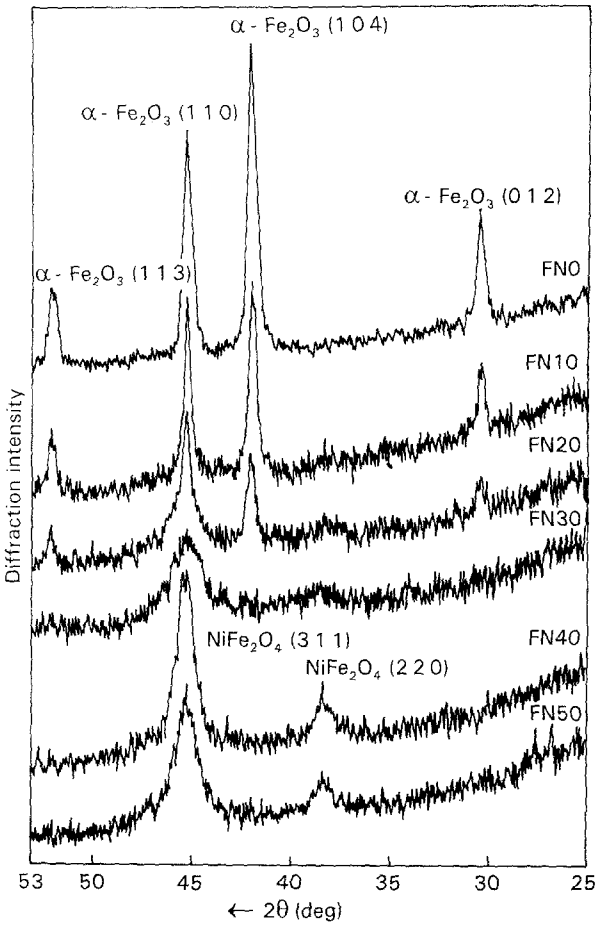

Figure 3 XRD powder patterns of iron–nickel mixed oxides heated at 550 °C.

spectrum is similar to that for FN50-1050 °C, although the peak positions are slightly different. There is no clear evidence for the presence of any alpha ferric oxide bands in the spectrum. The result reveals that the sample calcined at this temperature contains only the ferrite phase but probably with a different composition.

3.2. X-ray diffraction (XRD) analysis

XRD patterns of the mixed oxide samples heat treated at 550 °C for 1 h are shown in Fig. 3. The patterns of FNO, FN10 and FN20 have a number of alpha ferric oxide peaks. It should be noted that the (1 1 0) alpha ferric oxide peak coincides with the 100% intensity (3 1 1) nickel ferrite peak, and that the ferric oxide peaks gradually decrease in intensity with increasing nickel oxide content in the specimens. The intensity ratio of (1 1 0) to (1 0 4) peaks gradually increases with an increase in NiO up to 20 mol %, indicating that the proportion of alpha ferric oxide to nickel ferrite varies with NiO content in a sample. FN50 has peaks in the positions expected for nickel ferrite. The pattern of FN30 shows relatively broad and diffuse peaks indicating that the phases in this material are either amorphous or cryptocrystalline.

XRD patterns showed the presence of well-crystalline alpha ferric oxide and nickel ferrite when the mixed oxides containing up to 40 mol % NiO were calcined at 700 °C. These two phases co-exist together up to as high a temperature as 1300 °C for FN10, FN30 and FN40.

Diffraction patterns obtained from Debye–Scherrer powder photographs have shown both alpha ferric oxide and nickel ferrite lines for FN20 heat treated between 550 and 900 °C and sintered at 1200 and 1300 °C. On the contrary, the patterns of FN20 sintered at 1050 and 1100 °C contain only ferrite lines.

TABLE I The observed *d*-values (taken from Debye–Scherrer camera) and lattice parameters of FN20 and FN50 sintered at 1050 °C, along with standard ASTM values of nickel ferrite

Standard ASTM values of $NiFe_2O_4$			Observed *d*-spacings (nm)	
d(nm)	Intensity	*hkl*	FN50-1050 °C	FN20-1050 °C
0.4820	20	1 1 1	–	–
0.2948	30	2 2 0	0.2922	0.2901
0.2513	100	3 1 1	0.2499	0.2474
0.2408	8	2 2 2	0.2400	0.2377
0.2085	25	4 0 0	0.2075	0.2060
0.1913	4	3 3 1	–	–
0.1703	8	4 2 2	0.1698	0.1685
0.1605	30	5 1 1	0.1602	0.1590
0.1476	40	4 4 0	0.1473	0.1466
0.1319	6	6 2 0	0.1319	0.1313
0.1257	6	6 2 2	0.1258	0.1255
0.1204	6	4 4 4	0.1205	0.1205
0.1115	6	6 4 2	0.1115	–
0.1086	16	7 3 1	0.1086	0.1084
0.1042	6	8 0 0	0.1043	–
Lattice constant (nm) (error ± 0.0006 nm)		0.8339	0.8334	0.8307

Table I compares the d-values and lattice constants of FN20 and FN50 sintered at 1050 °C with those of the standard ASTM values of nickel ferrite. The lattice parameter value of 0.8307 nm obtained for FN20 is smaller than either the standard ASTM value for ferrite (0.8339 nm) or that of FN50 (0.8334 nm). Both i.r. and XRD results lead to the conclusion that a non-stoichiometric ferrite phase formed when FN20 was sintered near 1050 °C, which subsequently dissociated at higher temperatures to alpha ferric oxide and the stoichiometric nickel ferrite.

Further evidence for the formation of the non-stiochiometric ferrite has been obtained from measurements of magnetic susceptibility (χ_g), electrical conductivity (σ) and thermoelectric power (α).

3.3. Magnetic susceptibility (χ_g)

The room temperature susceptibility values plotted against the firing temperature of FN20 is shown in Fig. 4. Initially, the χ_g value gradually increased with temperature and reached a maximum at 1050 °C. The gradual change in χ_g has been attributed to the slow formation of the non-stoichiometric ferrite phase which is most probably completed ca. 1050 °C. The lower χ_g values observed for the specimens sintered at 1200 and 1300 °C, compared to FN20-1050 °C specimens, may be explained as due to the dissociation of the non-stoichiometric phase into alpha ferric oxide and stoichiometric ferrite above 1100 °C.

3.4. Electrical conductivity

Fig. 5 shows electrical conductivity plots of FN0, FN20 and FN50 sintered at 1050 °C. The FN20 specimen showed higher conductivity values than those of ferric oxide or nickel ferrite at all the measured temperatures. If FN20 is considered to be a composite containing both iron oxide and ferrite, it is expected that its conductivity plot should have been between the plots of FN0 and FN50. Conductivities of the materials at 125 °C are plotted as a function of sintering temperature in Fig. 6. Conductivity plots of both FN0 and FN50 gradually increased with sintering temperatures up to 1300 °C, this is attributed to the increased concentration of Fe^{2+} ions in the

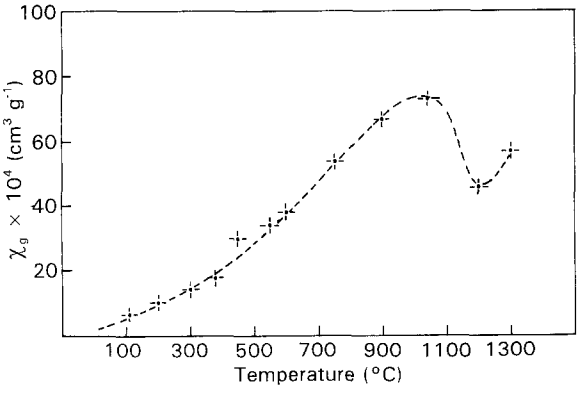

Figure 4 Magnetic susceptibility of the FN20 sample heat treated to different temperatures.

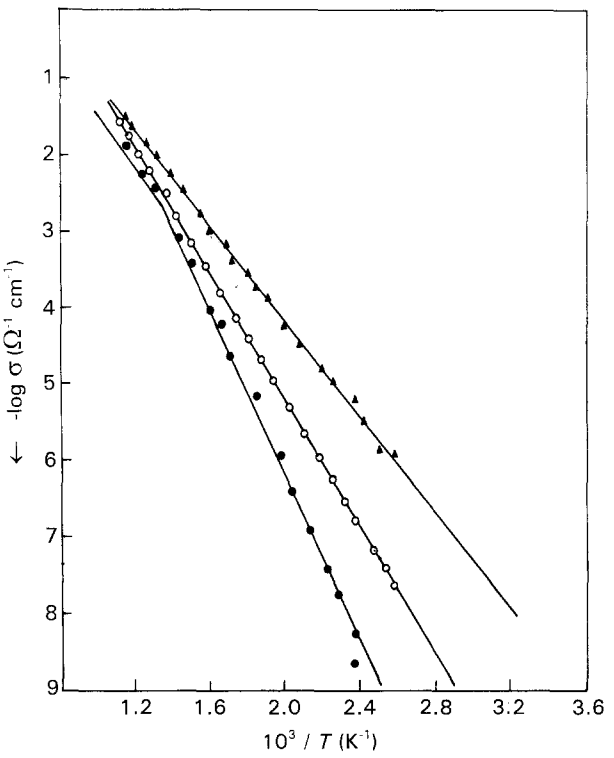

Figure 5 The electrical conductivity of mixed oxide specimens sintered at 1050 °C: FN0 (●), FN20 (△) and FN50 (○).

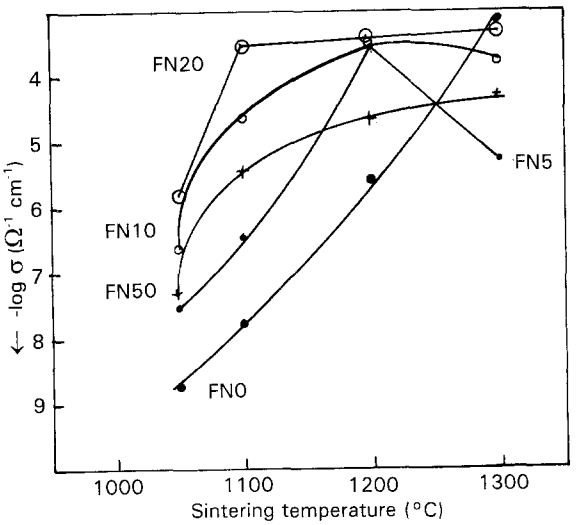

Figure 6 Electrical conductivity of iron–nickel mixed oxides at 125 °C sintered at different temperatures.

lattice. The conductivities of the other materials reached a maximum and then, with further increases of temperature, either remained constant (FN20) or decreased (FN5 and FN10). The changes in the conductivity values of these materials with sintering temperature are probably related to the presence of the non-stoichiometric ferrite phase which formed ca. 1050 °C for FN20 and dissociated to ferric oxide and nickel ferrite at higher temperatures.

3.5. Thermoelectric power

Both FN0 and FN50 sintered between 1050 and 1300 °C had negative thermoelectric power at all the

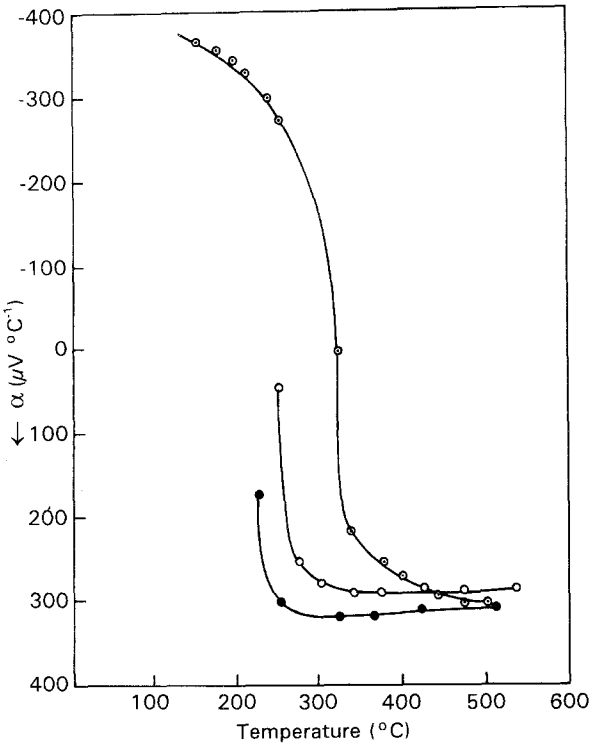

Figure 7 Thermoelectric power (α) of FN5 (●), FN10 (○) and FN20 (⊙) as a function of temperature. The specimens were sintered at 1050 °C.

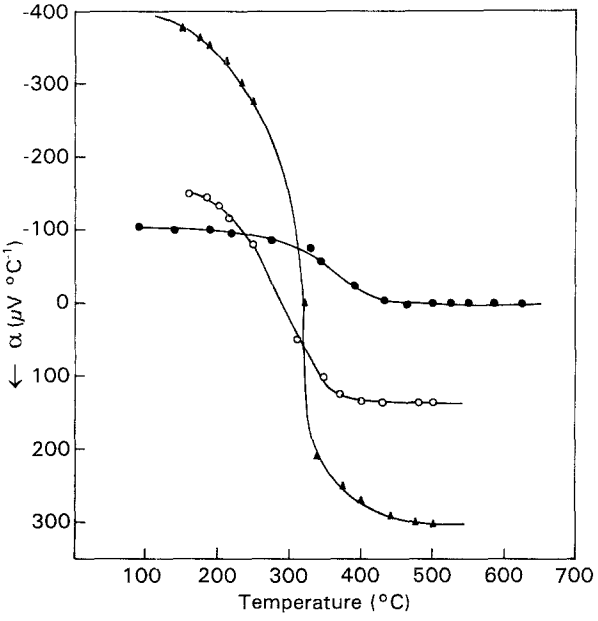

Figure 8 Thermoelectric power (α) of FN20 as a function of temperature sintered at 1050 °C (▲), 1200 °C (○) and 1300 °C (●).

measurement temperatures, indicating that the conduction in these materials was due to electrons [25]. The thermoelectric powers of these materials were almost independent of measurement temperatures. Thermoelectric power plots of FN20, FN10 and FN5 sintered at 1050 °C are given in Fig. 7. FN20 shows a very interesting temperature dependent behaviour, with a sharp change over of charge carriers at ca. 350 °C. The change over of charge carriers from electrons to holes observed for FN20 gradually decreased as the sintering temperature was increased to 1200 and 1300 °C (Fig. 8). Like FN20, the thermoelectric power of both FN5 and FN10 changed with measurement temperature (Fig. 7). However, data could not be obtained below 200 °C as the resistivity of the materials were too high.

4. Discussion

The anomalous nature of FN20 sintered close to 1050 °C is probably related to the presence of a non-stoichiometric ferrite spinel. This non-stoichiometric phase can be considered as either:

1. a solid solution between Fe_3O_4 and $NiFe_2O_4$ that has a general formula $[(Fe^{3+})_t(Fe^{3+}_{1-x}Ni^{2+}_xFe^{3+})_o]O_4$ (the Fe_3O_4 might be formed from the excess ferric oxide); or
2. a cubic gamma lacunar phase having a general formula $(NiFe_2O_3)_{1-x}$–$(\gamma$–$Fe_2O_3)_x$.

This gamma lacunar phase is a solid solution between nickel ferrite and γ-Fe_2O_3 and is considered as a superstructure having cation vacancies in the octahedral sites [7, 12–15].

Haematite dissociatively transformed to magnetite ($3Fe_2O_3 = 2Fe_3O_4 + 1/2O_2$) and the process depended both on the oxygen partial pressure (P_{O_2}) and the firing temperature. Also, the quantity of Fe_3O_4 retained in the material depended on the rate of cooling from high temperatures [26–30]. The reaction is reported to be completed at ca. 1400 °C in air [30]. In this investigation a non-stoichiometric phase was observed for FN20 that had been sintered at 1050 °C in air. Differential thermal analysis studies of FN20-550 °C had an endothermic peak at ca. 1310 °C, and that endotherm was associated with a weight loss of 1.65–1.85%. The cooling curve showed an exothermic peak at ca. 1120 °C with a gain in weight equivalent to that of the amount lost during heating. If the FN20-550 °C specimen is considered to be a mixture of 40 mol % $NiFe_2O_4$ and 60 mol % Fe_2O_3, the expected weight loss is ca. 1.69% for the complete conversion of ferric oxide to magnetite, which compares well with the experimentally observed weight loss. Therefore, to fabricate spinel solid solution of type (1) in air the mixed oxide samples containing an excess of ferric oxide need to be heat-treated at sufficiently high temperatures to covert Fe_2O_3 to Fe_3O_4 and then quenched rapidly in water or in liquid nitrogen to avoid re-oxidation of Fe_3O_4 to Fe_2O_3. However, at low P_{O_2}, the ferric oxide is almost fully transformed to magnetite at relatively low temperatures. For instance, a spinel solid solution has been detected in the O–Fe–Ni system containing 20 mol % Ni at a temperature as low as 700 °C when P_{O_2} was 10^{-14} [31].

Many investigators [32–34] have studied the electrical properties of the Fe_3O_4–$NiFe_2O_4$ system. Their results show that the system is highly conductive with the conductivity and activation energy values depending on the concentration of the Fe^{2+} ions in the system. Comparison of the reported conductivity and activation energy values [32–34] with the results of

FN20 (Fig. 5) revealed a notable difference. The activation energy of FN20-1050 °C was 0.63 eV, 2 to 3-times higher than the value reported for the spinel solid solution $[(NiFe_2O_4)_{1-x}-(Fe_3O_4)_x]$ having approximately the same composition [34]. Also, the change over of charge carriers from electrons to holes exhibited by FN20-1050 °C (Fig. 7) cannot be explained by considering the material as a solid solution between magnetite and nickel ferrite. Both resistivity and n–p anomalies, however, have been reported for pure and slightly substituted magnetite near the Verwey and Curie temperatures [34, 35].

The radius of the Fe^{2+} ion is larger than that of both Fe^{3+} and Ni^{2+} ions and accordingly the solid solution of Fe_3O_4 in $NiFe_2O_4$ will be followed by an expansion of the lattice ($a_{\text{magnetite}} - a_{\text{nickel ferrite}} = 0.006$ nm), while the solid solution of gamma ferric oxide in nickel ferrite will lead to a contraction of the ferrite lattice ($a_{\text{nickel ferrite}} - a_{\text{gamma ferric oxide}} = 0.003$ nm) [36]. In this study the lattice parameter of FN20-1050 °C was 0.8307 nm, 0.0027 nm lower than the lattice constant of FN50-1050 °C. This observation suggests that the FN20-1050 °C specimen can be considered as a solid solution between nickel ferrite and gamma ferric oxide. However, the presence of a some amount of Fe^{2+} ions (from magnetite) in the ferrite lattice cannot be discounted. The gamma lacunar phase is a superstructure having cation vacancies which can trap holes [16, 37].

The change over of charge carriers from electrons to holes at ca. 350 °C for FN20-1050 °C (Fig. 7) suggests that both n- and p-type charge carriers are present in the structure. Therefore, conduction should be mixed and will be dominated by either electrons or holes depending on the concentration and mobility of the species at a particular temperature. Electronic conduction is expected to be dominant at low temperatures, as electron mobility is higher than hole mobility. The thermoelectric power of FN20-1200 °C was relatively less sensitive to measurement temperature, and FN20-1300 °C had only a negative thermoelectric effect at all measurement temperatures (Fig. 8), indicating that the non-stoichiometric ferrite phase formed at 1050 °C was mainly responsible for this change over behaviour.

The conductivity and thermoelectric power results of FN5 and FN10 can be explained by considering that the ferrite phase present in these materials is a non-stoichiometric one probably similar to that of FN20-1050 °C. Since this phase is more conducting than the alpha ferric oxide, the overall conductivity of the specimen increases with increasing amounts of NiO as consequence of increasing fractions of the non-stoichiometric phase.

5. Conclusions

In conclusion it may be stated that formation of a non-stoichiometric ferrite phase occurs when the FN20 specimen is sintered near 1050 °C. This phase is stable only over a limited range of temperatures and dissociates into alpha ferric oxide and nickel ferrite above 1200 °C. The conductivity of this phase is higher than either alpha ferric oxide or stoichiometric nickel ferrite, and its thermoelectric power is strongly dependent on temperature.

Acknowledgements

The authors wish to thank Dr M. J. Bannister, CSIRO, Materials Science and Technology Division, Clayton, Victoria, Australia, for reviewing the manuscript and Dr H. S. Maiti, CGCRI, Calcutta, India, for his help at various times.

References

1. E. W. GORTER, *Philips Res. Rep.* **9** (1954) 295.
2. G. BLAZZE, *Philips Res. Rep. Suppl.* (1964).
3. J. B. GOODENOUGH, in "Magnetism and chemical bonds" (John Wiley and Sons, New York, 1976).
4. M. PAULUS, in "Preparative methods in solid state chemistry", edited by Hagen Muller (Academic Press, London, 1972) p. 587.
5. D. J. CRAIK, in "Magnetic oxides, Part 1", edited by D. J. Craik (John Wiley, New York, 1975) p. 67.
6. M. H. LEWIS, *Phil. Mag.* **20** (1969) 985.
7. T. YAMAGUCHI and T. KIMURA, *J. Amer. Ceram. Soc.* **59** (1976) 333.
8. A. H. HEUER and T. E. MITCHELL, in "Precipitation process in solids", edited by K. C. Russell and H. T. Aaronson (Metals Society of the AMIE, Warrendale, PA, 1978).
9. W. T. DONLON, T. E. MITCHELL and A. H. HEUER, *J. Mater. Sci.* **17** (1982) 1389.
10. D. M. ROY, R. ROY and E. F. OSBORN, *J. Amer. Ceram. Soc.* **36** (1953) 149.
11. H. JAGODZINSKI and H. SAALFIELD, *Z. Kiristallog.* **110** (1958) 197.
12. B. GILLOT, J. TYRONOMICZ and A. ROUSSETT, *J. Mater. Res. Bull.* **10** (1975) 775.
13. F. CHASSAGNEUX and A. ROUSSET, *J. Solid State Chem.* **16** (1976) 161.
14. B. GILLOT, F. BOUTON, J. F. FERRIOT, F. CHASSAGNEUX and A. ROUSSET, *J. Solid State Chem.* **21** (1977) 375.
15. B. GILLOT, R. M. BENLOCIF and A. ROUSSET, *J. Solid State Chem.* **38** (1981) 219, **39** (1981) 329.
16. B. GILLOT and F. JEMMALI, *Phys. State. Sol.* (a) **76** (1983) 601.
17. S. RAJENDRAN, PhD thesis, IIT, Kharagpur, India (1983).
18. A. A. IBAHIM and G. A. EL-SHOBAKY, *Thermochim. Acta* **132** (1988) 117.
19. Y. TAMAURA, T. SASAO and T. ITOH, *J. Colloid Interface Sci.* **136** (1990) 242.
20. K. D. J. MacKENZIE and C. M. CARDILE, *Thermochim. Acta* **165** (1990) 207.
21. M. LENGLET, R. GUILLAMET, J. LOPITAUX and B. HANNOYER, *Mater. Res. Bull.* **26** (1991) 575.
22. S. MUSIC, S. POPOVIC and S. DALIPI, *J. Mater. Sci.* **28** (1993) 1793.
23. S. RAJENDRAN, V. SITAKARA RAO and H. S. MAITI, *J. Solid State Chem.* **53** (1984) 227.
24. P. TARTE and J. PREUDHOMME, *Spectrochim. Acta* **29A** (1973) 1301.
25. H. S. MAITI, S. RAJENDRAN and V. SITAKARA RAO, *Phys. Status Solidi (a)* **84** (1984) 631.
26. R. N. BLUMENTHAL and D. H. WHITE, *J. Amer. Ceram. Soc.* **44** (1961) 508.
27. G. G. CHARETTE and S. N. FLENGAS, *J. Electrochem. Soc.* **115** (1968) 796.
28. P. E. C. BRYANT and W. W. SMELTZER, *J. Electrochem. Soc.* **116** (1969) 1409.
29. M. ISHII, M. NAKAHIRA and T. YAMANKA, *Solid State Commun.* **11** (1972) 209.

30. J. H. DE WIT, A. F. BROERSMA and STROBAND, *J. Solid State Chem.* **37** (1981) 242.27
31. A. D. PELTON, H. SCHMALZRIED and J. STICHER, *J. Phys. Chem. Solids* **40** (1979) 1103.
32. Y. MIYATA, *J. Phys. Chem. Jpn* **16** (1961) 206.
33. A. A. SOMOKHVALOV and A. G. RUSTAMOV, *Soviets Phys. Solid State* **7** (1965) 961.
34. B. A. GRIFFITHS, D. ELWELL and R. PARKER, *Phil. Mag.* **22** (1970) 163.
35. T. YAMADA, *J. Phys. Soc. Jpn* **38** (1975) 1378. 30.
36. C. OKAZAKI, *J. Phys. Soc. Jpn* **15** (1960) 2013.
37. P. S. JAIN and V. S. DARSHANE, *Indian J. Chem.* **19A** (1980) 1050.

Received 13 July 1993
and accepted 21 April 1994